

Composite Mølmer-Sørensen gate

K. N. Zlatanov,^{1,2} S. S. Ivanov,¹ and N. V. Vitanov¹

¹*Center for Quantum Technologies, Department of Physics,
Sofia University, James Bourchier 5 blvd., 1164 Sofia, Bulgaria*

²*Institute of Solid State Physics, Bulgarian Academy of Sciences, Tsarigradsko chaussée 72, 1784 Sofia, Bulgaria*

(Dated: February 11, 2025)

The Mølmer-Sørensen (MS) gate is a two-qubit controlled-phase gate in ion traps that is highly valued due to its ability to preserve the motional state of the ions. However, its fidelity is obstructed by errors affecting the motion of the ions as well as the rotation of the qubits. In this work, we propose an amplitude-modulated composite MS gate which features high fidelity robust to gate timing, detuning and coupling errors.

I. INTRODUCTION

Ion traps are one of the leading platforms for quantum information [1, 2], simulation [3, 4] and sensing [5, 6]. For the past two decades these devices have excelled in single and two-qubit gate fidelity. Single qubit gates have achieved error rates as low as 1.5×10^{-6} [7] and even 10^{-7} [8], while two-qubit gate errors are currently of the order of 10^{-4} [9, 10]. Although such fidelity is below the fault tolerance limit the need for further improvements in it is ever present, since error correction is in general a resource-heavy procedure.

Standard ion traps employ spin-motion coupling to transmit interactions and hence they are prone to heating. The latter has a detrimental effect on the gate's fidelity and requires periodic cooling procedure. Among the different two-qubit gates proposed, the Mølmer-Sørensen (MS) gate [11, 12] is highly cherished for its ability to preserve the motional state of the ions and thus avoid heating. The preservation of the motional state is caused by the path interferences induced by bichromatic excitation on both sidebands. This interference remains not only for pure Fock states but also for coherent states [13]. Experimentally it was first demonstrated more than 20 years ago [14], and more recently implemented on a chip surface traps [15], which outlines its efficiency and universality. The employed mechanism has also been investigated for other platforms like cavity QED [16] as well as in neutral atoms [17]. Possible applications in Rydberg ions can be considered for the mitigation of motional effects over the gate's fidelity.

The MS gate, however, is susceptible to various errors stemming from imperfect laser settings, interactions with the environment, cross-talk and miscalibration, which can be categorized as motional and rotational errors, based on which component of the propagator they affect. A number of techniques for the suppression and mitigation of these errors have been developed and experimentally demonstrated. For example, multi-tone excitation has shown mitigation of errors caused by heating of the motional mode [18], as well as resilience versus gate timing errors and errors in the frequency of the motional mode [19]. Pulse-shaping demonstrated resistance to disturbances of the motional mode [20]. Ampli-

tude modulation proved robustness towards normal mode frequency fluctuations [21]. Frequency modulation techniques have been developed against static offsets of the motional-mode frequencies [22, 23]. Phase modulations have shown robustness towards laser amplitude and gate detuning errors [24]. Most of these techniques correct for a single type of errors, therefore the question of combining techniques in order to correct for multiple errors simultaneously arises naturally.

In this paper, we propose the combination of amplitude modulation and composite pulses as a promising strategy to suppress multiple errors at once. This combination of techniques has been proposed earlier in a different context [27]. Composite MS gates have been proposed previously in [28] under the strong assumption that errors only occur in the rotational component of the gate. This assumption can hardly be met experimentally, since the control parameters that are quite probable to be the source of the errors like the Rabi frequency, the detuning and the timing of the gate affect both components. We demonstrate below that when such errors are accounted for in the motional component of the gate, the composite MS sequence can actually worsen its fidelity compared to a single gate. We show, however, that when combined with the proper amplitude modulation, composite MS gates can outperform not only the standard MS gate configuration but also the multi-tone excitation schemes.

This paper is organized as follows, Section II introduces the dynamics of the MS gate. Section III discusses amplitude modulation and composite sequences. In Section IV we demonstrate the results through numerical simulations, and we conclude in Section V.

II. DYNAMICS OF THE MS GATE

The bichromatic excitation of the first red and blue sidebands of two trapped ions is described by the Hamiltonian

$$H = g \sum_k \sigma(\zeta_k^+) \left(a^\dagger e^{i\epsilon t - i\zeta_k^-} + a e^{-i\epsilon t + i\zeta_k^-} \right), \quad (1)$$

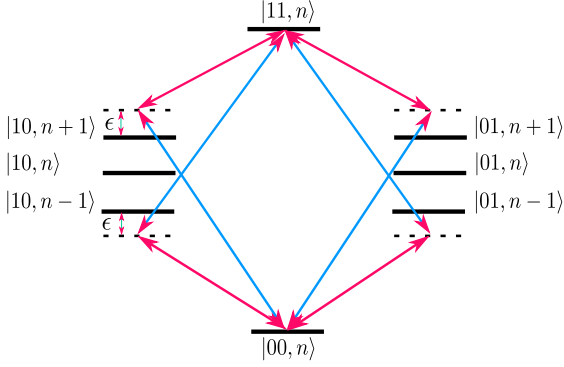


Figure 1. (Color online) Excitation scheme of the Molmer-Sorensen gate. A combination of red and blue side-band excitation on each ion create an interference excitation path which allows a decoupling between the motional and spin degrees of freedom. The laser fields must be slightly detuned by ϵ from the photon-phonon resonance.

where $\zeta_k^\pm = \frac{1}{2}(\zeta_k^b \pm \zeta_k^r)$ is composed of the blue and red sideband phases, ϵ is the photon-phonon detuning to the intermediate state, $g = i\Omega\eta/2$ is the effective coupling and $\sigma(\zeta_k^+) = \sigma_k^+ e^{-i\zeta_k^+} + \sigma_k^- e^{i\zeta_k^+}$ are the spin operators. The simplified linkage pattern this Hamiltonian creates is illustrated in Fig. 1.

The propagator associated with Eq. (1) can be found by calculating the first two terms (all others vanish) of the Magnus expansion,

$$M_1(t) = -\frac{i}{\hbar} \int_0^t H(t_1) dt_1, \quad (2a)$$

$$M_2(t) = \frac{1}{2} \left(\frac{i}{\hbar} \right)^2 \int_0^t \int_{t_1}^{t_2} [H(t_1), H(t_2)] dt_2 dt_1, \quad (2b)$$

and reads

$$U_{MS} = D(\alpha) e^{i\theta(t)\sigma(\zeta_1^+)\sigma(\zeta_2^+)}, \quad (3)$$

where the displacement operator is given as

$$D(\alpha) = \exp \left\{ \sum_k \sigma(\zeta_k^+) [\alpha_k(t) a^\dagger - \alpha_k(t)^* a] \right\}. \quad (4)$$

The functions

$$\alpha_k(T_1, T_2) = -i \int_{T_1}^{T_2} g(\tau) \exp(i\epsilon\tau - i\zeta_k^-) d\tau, \quad (5a)$$

$$\theta(T_1, T_2) = 2 \int_{T_1}^{T_2} \int_{T_1}^{\tau_2} g(\tau_1) g(\tau_2) \sin(\epsilon(\tau_1 - \tau_2)) d\tau_1 d\tau_2, \quad (5b)$$

govern the evolution of the system. For example, if we wish to generate $|\Phi^+\rangle = \frac{1}{\sqrt{2}}(|00\rangle + |11\rangle)$ we require $\alpha(\tau_g) = 0$ and $\theta(\tau_g) = \pi/4$ at the gate time. This introduces a number of constraints between the control parameters.

For example, if standard constant coupling is employed, then

$$\epsilon = 4g, \quad (6a)$$

$$t\epsilon = 2\pi. \quad (6b)$$

Errors stemming from a variety of sources can cause an incomplete trajectory in phase space or miss the gate time τ_g . For the vast majority of errors these two effects can happen simultaneously. This is a direct consequence of the model-specific parameter relations that arise, like the ones of Eqs. (6). If an error occurs in one of the parameters it affects the relations to the others and thus lowers the fidelity. It is tempting to assume that errors emerge systematically in different parameters, say $t \rightarrow t(1 + \delta)$ or $\epsilon \rightarrow \epsilon(1 + \delta)$, where δ is the error. However, this is not the case and thus mitigation strategies aimed at fixing one can not always be used for the other, as we show in the next section. The protocol we propose aims to mitigate errors in the control parameters, ϵ , g and τ_g , and thus to achieve a high fidelity gate even though the model-specific relations between the parameters may not hold.

One of the popular techniques for error mitigation is the multi-tone excitation, which relies on adding a number of laser beams shifted in frequency. The Hamiltonian of Eq. (1) is then transformed to [18]

$$H_{MT} = \sum_k \sigma(\zeta_k^+) \sum_{j=1}^n g_j \left(a^\dagger e^{ij\epsilon t - i\zeta_k^-} + a e^{-ij\epsilon t + i\zeta_k^-} \right), \quad (7)$$

where j runs over the added tones and g_j is given as -0.1444ϵ and 0.2888ϵ [25] for $j = 1$ and $j = 2$, respectively. Usually only the first two tones are used, since experimentally adding enough power to the different tones is challenging [26]. Due to the popularity of this technique we will use it as a reference point to which we will compare our protocol. For that purpose we will use the infidelity, defined as $1 - F$, as a measure. Here the fidelity reads,

$$F = \frac{1}{K} \text{Tr}(U_t^\dagger U_{err}), \quad (8)$$

with K being the number of states, U_t is the target propagator, while U_{err} is the propagator in which an error in any of the parameters $s \rightarrow s(1 + \delta)$ has occurred.

III. AMPLITUDE MODULATION AND COMPOSITE GATES

In this section we introduce the techniques of amplitude modulation and composite pulses for two-qubit gates. Ultimately our goal is to combine them and keep their benefits while diminishing their flaws. We will employ amplitude modulation for its ability to mitigate timing and detuning errors and we will also join together multiple gates, generating a sequence, mimicking composite pulses techniques, to eliminate rotational errors.

A. Amplitude modulation

In order to find a proper time-dependent Rabi frequency which will be able to produce the MS gate, there are a couple of assumptions we can make based on Eqs. (2). First, we demand that the $M_1(t)$ term evaluates to 0 at the gate time which will ensure a closed trajectory in the phase space. Second, due to the form of the $M_2(t)$ term, the Rabi frequency must have a good auto-correlation in order to achieve a strong excitation with minimal amount of power. Both of these assumptions have to be satisfied simultaneously. A natural candidate functions that satisfy these requirements are the trigonometric functions. Using a sine function provides a smooth-start [29], which minimizes the coupling to the carrier and also has proven to have a low power requirement [20]. In order to find a larger family of functions, we can combine it with a cosine of a certain degree, as long as the smooth start is ensured. In its most general form the coupling of Eq. (1) then reads

$$g(t, m, l, n, p) = A \sin(mt)^l \cos(nt)^p. \quad (9)$$

Such amplitude modulation provides analytical expressions for $\alpha(t)$ and $\theta(t)$, for all different sets of parameters m, l, n, p . They are too cumbersome to be presented here so instead we demonstrate the dynamics of a few of these modulations shown Fig. 2. We present their analytical form used for this illustration in the Appendix.

These modulations generate a variety of trajectories, illustrated in Fig. 2(b), some quite similar and others quite different. The relation between the phase space trajectory and the robustness versus specific parameter is not fully understood. There are empirical observations which state that on average the trajectory must be as close to the center as possible. A strict mathematical derivation describing the relation between robustness and trajectory is yet to be derived. We note that there are attempts to achieve this with an interesting algebraic approach [20].

We now turn our attention to the selected modulations and point out that since the parameter space is quite rich the following discussion is not aimed at drawing the borders of the best performing parameter region, but rather to draw quantitative conclusions based on the given examples. For example, the sine-squared shape modulation is in general quite good for gate timing errors, as it transforms the point of entanglement into a plateau. Changing the frequency of the sine also seems to impact the infidelity, as can be seen from Fig. 2(c).

When we look at the performance against detuning errors, shown in Fig. 2(d), we see that the $\sin(t/2)^2 \cos(t)$ outperforms the other sine shapes. Note the asymmetry in Fig. 2(d), which is due to a “forbidden trajectory”, that is a trajectory whose detuning values make the corresponding $\alpha(t)$ function go to infinity. In this example of amplitude modulation a larger detuning is required so that a closed trajectory can be formed and consequently a stronger coupling is needed. Thus a clear trade-off emerges between gate-time, power and robust-

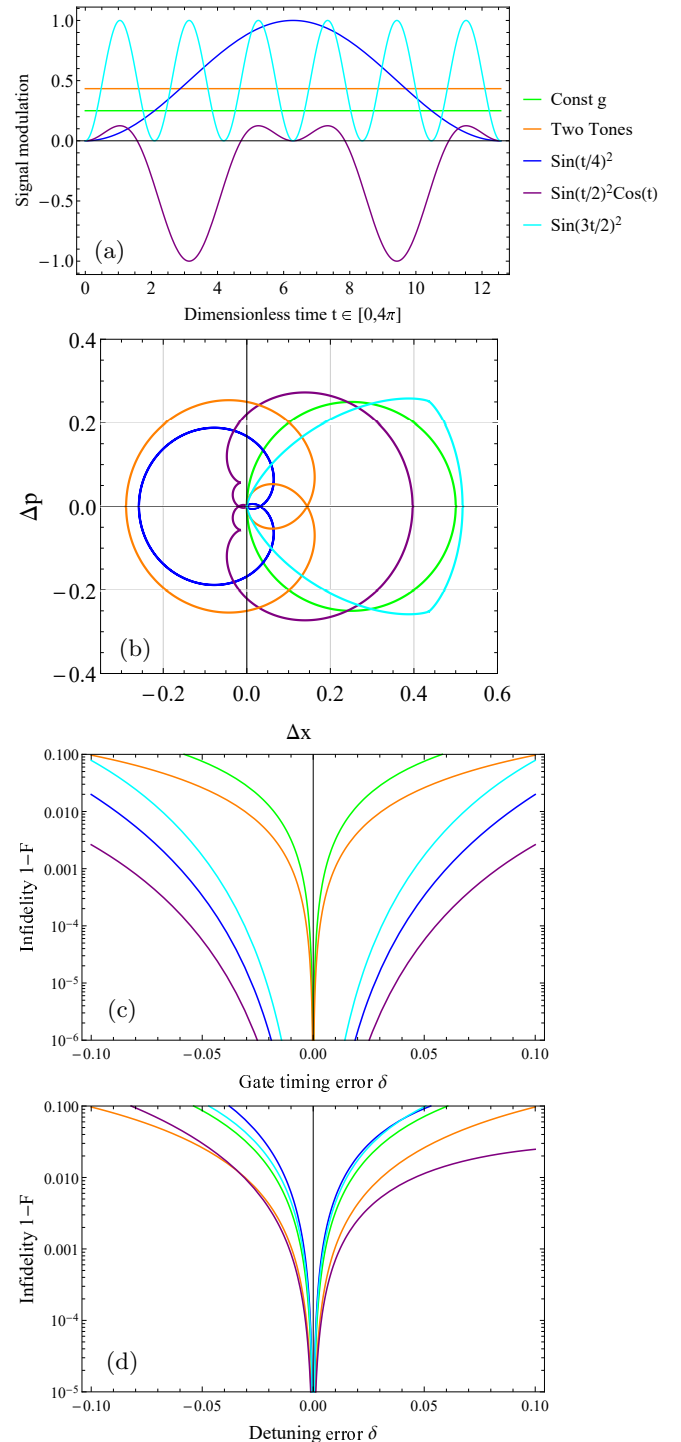


Figure 2. (Color online) MS gate under sine amplitude modulation. Frame a) shows the used signals for amplitude modulation and frame b) illustrates the phase space trajectories. Frames c) and d) depict the infidelity for gate timing and detuning errors respectively. The simulations were carried on the first possible trajectory for integer detuning, which for the order given in frame a) reads $\epsilon \rightarrow \{1, 1, 1, 3, 1\}$ in units of τ_g^{-1} with the corresponding gate times and couplings given as $\tau_g \rightarrow \{2\pi, 2\pi, 4\pi, 2\pi, 2\pi\}$ and $g \rightarrow \{0.25, 0.433, 0.2733, 0.85, 0.516\}$ in corresponding units of frequency. All simulations are done with 14 motional states.

ness to multiple parameters, that one has to keep in mind, when choosing a specific modulation signal with respect to the experimental platform at hand. In our simulations we use only two-tone excitation optimized for detuning errors, and for that reason it gains infidelity versus gate timing errors. We also point, however, that it can be optimized for gate timing errors as in Ref. [19]. We see that for detuning errors the sine-cosine modulation can underperform or outperform the multi-tone excitation depending on the sign of the detuning error. In any case it is more advantageous to use such amplitude modulation since it also provides gate timing robustness. We will use it in a composite sequence in order to generate a gate that is robust against any type of error. As well as the other two signals, namely the $\sin(t/4)^2$ and the $\sin(3t/2)^2$ modulations. Thus we attempt to draw any conclusion about their performance based on their phase-space trajectory, as the former provides quite a different trajectory than the multi-tone excitation, while the later has its trajectory quite similar. In terms of fidelity the former performance is somewhat in the middle of all other shapes, while the later has the worst performing infidelities for gate timing errors. It is worthwhile to point out that these two modulations behave even worse than the standard gate versus detuning errors, and it is crucial to clarify that this behavior is due to the phase-space trajectory, which we can also change by the detuning, rather than the modulation itself.

B. Composite gates

The idea of making a composite MS gate was first proposed in Ref. [28] and we refer the reader to this reference for a detailed derivation of the proposed sequences as well as any other details. Here we will only briefly introduce the procedure of generating robust composite MS gate. It uses the sequence

$$U^{(N)}(\theta) = F(\phi_{N+1})U(\theta_N)F(\phi_N) \cdots U(\theta_0)F(\phi_0), \quad (10)$$

where,

$$U(\theta) = e^{i\theta\sigma_x\sigma_x}, \quad (11a)$$

$$F(\phi) = e^{-i\phi\sigma_z}. \quad (11b)$$

Such a sequence can be robust to rotational errors in the angle θ by a proper choice of the individual rotation angles θ_N and the phases of the $F(\phi_N)$ gates. The phase gates can be incorporated in the rotational gates by introducing

$$U_\phi(\theta) = e^{i\theta\sigma_x\sigma(\phi)}, \quad (12)$$

where $\sigma(\phi) = \sigma_x \cos \phi + \sigma_y \sin \phi$. Eq. (10) then can be rewritten as

$$U^{(N)}(\theta) = F(\phi_{N+1}) \prod_{k=0}^N U_{\phi_k}(\theta_k) \quad (13)$$

In this manner broadband sequences can be generated if we make sure that

$$\frac{\partial^l}{\partial \delta^l} \left[U^{(N)}(\theta) - U(\theta) \right] \Big|_{\delta=0} = 0 \quad (14)$$

is satisfied, where l denotes different orders of correction.

The propagator of Eq. (12) differs from Eq. (3) by the displacement operator. We can control the sign of the displacement α with the $\zeta_1^- = \zeta_2^- = \zeta^-$ phases. In this manner we can revert the displacement operator with two consecutive gates if we can ensure that $D(-\alpha)D(\alpha) = \mathbf{1}$. This can happen if they have the same ζ_k^+ phases, and also we choose the ζ^- phase of every second gate such that the relation

$$D(\alpha(\zeta^-)) D(\beta) = e^{\frac{\alpha(\zeta^-)\beta^* - \alpha^*(\zeta^-)\beta}{2}} D(\alpha(\zeta^-) + \beta) = \mathbf{1} \quad (15)$$

will hold. This means that each logical gate in the sequence has to be represented by two physical gates that cancel each others displacement and rotate at half the angle as

$$\begin{aligned} U_\phi(\theta)_{\text{logic}} &= \underbrace{e^{i\frac{1}{2}\theta(t_2)\sigma_x\sigma(\zeta_2^+)} D(-\alpha)}_{\text{2nd gate}} \underbrace{D(\alpha)}_{\text{1st gate}} e^{i\frac{1}{2}\theta(t_1)\sigma_x\sigma(\zeta_2^+)} \\ &= e^{i\theta\sigma_x\sigma(\zeta_2^+)}, \end{aligned} \quad (16)$$

where t_1 and t_2 account for the proper time intervals of the gates. The phase ζ_2^+ corresponds to ϕ , and is present in both the displacement and the rotational part of the propagator, thus we will always set $\zeta_1^+ = 0$ and control the rotation by the phase ζ_2^+ .

The shortest sequence we can employ consists of three logical gates [28] and one single qubit phase gate,

$$\mathbf{B}_1(\theta) = F(-2\phi) \left(\frac{\pi}{2}\right)_{3\phi} \left(\frac{\pi}{2}\right)_\phi (\theta)_0, \quad (17)$$

where the sequence acts from right to left, that is the $(\theta)_0$ gate is implemented first. This sequence however underperforms against gate timing errors (see Fig. 3) for both constant and modulated signal. In our simulations of composite sequences we assume that timing errors will affect only the last physical gate in the sequence. The reason for this assumption is that generating a sequence of pulses with an acousto-optical modulator(AOM) is quite precise in the timing between individual pulses. Thus we assume that the timing error is caused by a shutter that opens or closes prematurely, and in this way cuts short the last physical gate or prolongs it. In this scenario, the error in the $\mathbf{B}_1(\theta)$ sequence will also affect the single qubit phase gate. Also, depending on the modulation signal, it might not preserve the plateau of the gate region, losing the advantage of amplitude modulation. In order to avoid that we will use a permuted version, which performs better, namely

$$\mathbf{B}_2(\theta) = (\theta)_0 \left(\frac{\pi}{2}\right)_\phi \left(\frac{\pi}{2}\right)_{3\phi} F(2\phi). \quad (18)$$

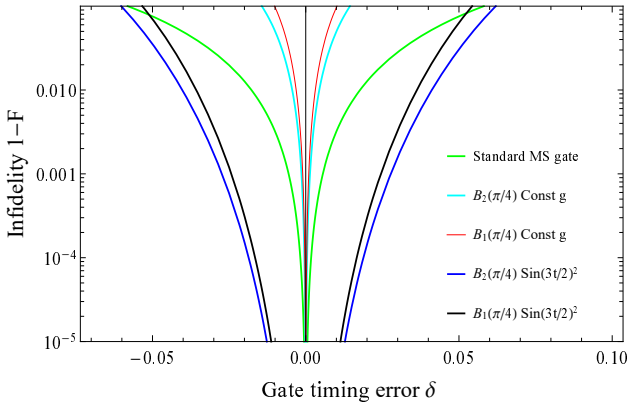


Figure 3. (Color online) Infidelity versus gate timing error for $\mathbf{B}_1(\pi/4)$ and $\mathbf{B}_2(\pi/4)$ with constant signal (cyan and red lines) and for $\sin(3t/2)^2$ modulation (blue and black lines), compared to a standard MS gate. All sequences account for errors in the displacement operator as well. All sequences span an equally divided time interval of 2π , the detuning is $\epsilon = 1 [\tau_g^{-1}]$ and the couplings are set such that the required rotation for each gate in the sequence is achieved.

In this sequence the rotating gate comes last and this ensures that the timing error will not affect any other gate in the sequence and also that any robustness of the modulation will be inherited by the sequence. Although longer sequences will compensate for higher-order errors, they can also increase the gate time. Even the sequence of Eq. (18) can be longer by a factor of 2 to 3 than the single MS gate, depending on the employed modulation and the available power. Hence we will limit ourselves only to short sequences like $\mathbf{B}_2(\theta)$. The phase gate in these sequences is on the second qubit and the phases are set to $\phi = \arccos(-\theta/\pi)$.

IV. COMPOSITE GATES WITH AMPLITUDE MODULATION

In this section we present the main result, which is the infidelity of the $\mathbf{B}_2(\theta)$ sequence for different amplitude modulations compared to the standard and the two-tone MS gate.

The robustness of the sequence is mostly affected by the trajectory in phase space each individual propagator creates, although each two consecutive gates will revert the motion back to its original state. The modulation of the signal and the detuning play a critical role for the form of the phase space trajectory. We stick to our rule to employ the trajectory generated on the first possible integer of the detuning. This is illustrated in Fig. 4 for the sequence of Eq. (18). In frame a), we see that all amplitude modulated sequences outperform the standard and the two-tone gate versus the gate timing error, an expected result, since the standard gate is not robust towards a timing error and we use a two-tone gate which is optimized for detuning errors. In frame b), we see

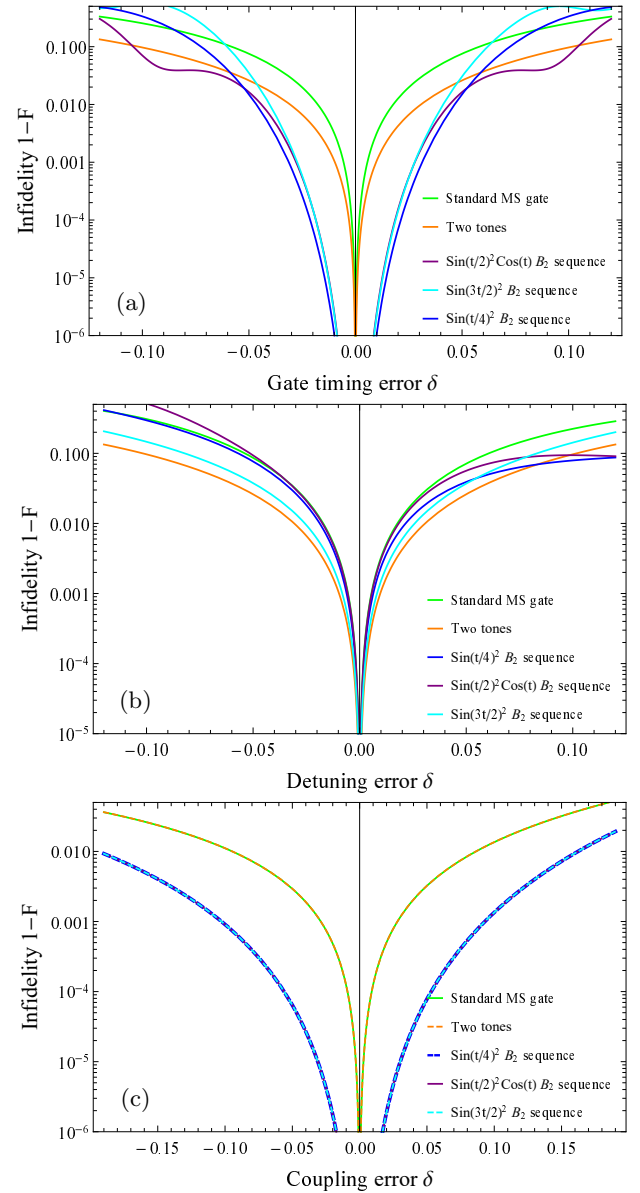


Figure 4. (Color online) Infidelity versus error from specific source. Frame a) shows infidelity vs gate timing errors, frame b) versus detuning error, and frame c) versus coupling error. The ζ^- phase that revert the displacement on every second gate in the sequence for the $\sin(t/4)^2, \sin(3t/2)^2, \sin(t/2)^2 \cos(t)$ read $\{0, -\pi + 0.6207, 0\}$ respectively. The detuning reads $\epsilon \rightarrow \{1, 1, 3\} [\tau_g^{-1}]$, and the gate times are $\tau_g \rightarrow \{6\pi, 2\pi, 12\pi\}$.

that, for the given trajectories the different amplitude modulations are all better than the standard gate versus detuning error, but only the $\sin(3t/2)^2$ modulation performs comparably to the two-tone implementation of the gate. Now this is unexpected based on the individual performances of the modulations as we see in Fig. 2 d), where it was worse than the two-tones, and only the sine-cosine modulation was performing comparably. In frame c) we see that the standard and the two-tone im-

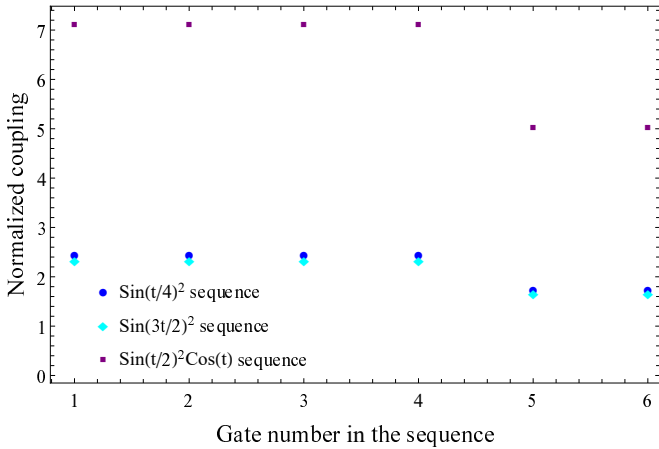


Figure 5. (Color online) Coupling strength of each gate in the sequence normalized to the coupling of a single MS gate of the specific modulation.

plementations have the same resilience to coupling errors, while the performance of each modulation is the same. This is because the robustness towards coupling errors is independent of the modulation, whenever a composite sequence is employed, and is due to the sequence itself.

Based on the given examples the $\text{sin}(3t/2)^2$ modulated sequence gives the best result in terms of multi-error robustness and is as long as the standard MS gate. The reasons for this is related to its trajectory and also to its fast oscillation during the sequence time ($t \in [0, 2\pi]$). This modulation has three symmetrical peaks and this allows the implementation of all phases in the peaks of the field. In this way each gate in the sequence can be realized within a half-period of the signal. For the same reason both $\text{sin}(t/4)^2$ and $\text{sin}(3t/2)^2$ sequences were given enough time (12π and 6π), also such that each logical gate constitutes a period of the modulation. The power costs per gate for each modulation is illustrated in Fig. 5 where each gate of the sequences is normalized to the coupling strength that a single MS gate needs for the specific modulation. The $\text{sin}(3t/2)^2$ has the lowest power requirements, which again supports our claim that it is very suitable modulation for composite MS gate. All presented modulations require larger power for each gate in the sequence than the minimal power required for the single modulated gate, which is to be expected since we are forcing the same rotation for a shorter time period (say $\pi/4$ over $\tau_g/6$). This power requirement can be relaxed if we simply allow a slower gate, that is, a longer time interval for each gate in the sequence.

V. DISCUSSION AND CONCLUSION

In this work we presented the combined technique of amplitude modulation and composite gates to produce a

Molmer-Sorensen gate which is robust to timing errors, rotational errors and detuning errors. To our knowledge, the sine-cosine amplitude modulation is new and individually it performs quite well against both timing and detuning errors. The permuted sequence of Eq. (18) that we propose negates the effects of errors propagation from the two-qubit part of the sequence to the single-qubit gates in it and maintains the robustness of the amplitude modulation versus gate timing errors. The $\text{sin}(3t/2)^2$ modulated sequence outperforms the two-tone excitation technique versus all types of errors except for an error in the detuning, although its performance there is quite similar. It also surpassed the sine-cosine modulation, which performs better individually. Based on that we can conclude that the best performing modulation individually is not necessarily the best performing modulation in a sequence. Furthermore, the $\text{sin}(t/4)^2$ modulation's trajectory is very similar to the two-tone's trajectory, yet their performances, both individually and in a sequence, differ strongly. Thus a clear indication for the performance of a MS gate, based only on its phase-space trajectory can not be derived. There is a clear trade-off between time, power and robustness which is an expected effect, also observed in single qubit gates [30]. In general, the power costs of a sequence with modulated Rabi frequency are a bit below 2.5 times the cost of a single MS gate with the same modulation. Different modulations allow for a variety of gate times ranging from the minimal gate time for a single MS gate to a few multiples of it. However, choosing a proper signal for modulation in a composite gate has to be in accordance with the power capabilities of the implementing platform and its individual tolerances to errors of different nature.

ACKNOWLEDGMENTS

This research is supported by the Bulgarian national plan for recovery and resilience, Contract No. BG-RRP-2.004-0008-C01 (SUMMIT), Project No. 3.1.4 and by the European Union's Horizon Europe research and innovation program under Grant Agreement No. 101046968 (BRISQ).

Appendix A: Analytical expressions for α and θ

Here we provide analytical expressions for the functions of Eqs.(5). We only show them for a time interval in which a rotation of $\pi/4$ is achieved and we have set all phases to 0 for simplicity. Starting with the $\text{sin}(t/4)^2$ modulation for $t \in [0, 4\pi]$ they read,

$$\alpha(t) = \frac{g}{2\epsilon(4\epsilon^2 - 1)} \left[e^{it\epsilon} \left(4\epsilon^2 \cos(t/2) - 2i\epsilon \sin(t/2) - 4\epsilon^2 + 1 \right) - 1 \right], \quad (\text{A1a})$$

$$\theta(t) = -\frac{g^2}{2(\epsilon - 4\epsilon^3)^2} \left[24t\epsilon^5 - 10t\epsilon^3 + 2(4\epsilon^2 - 1)\epsilon^3 \sin(t) + 4\epsilon^2 \sin(t\epsilon) - 4\epsilon^2 \cos(t/2) \sin(t\epsilon) \right. \\ \left. - 2\epsilon \sin(t/2) \left(1 - \cos(t\epsilon) + 32\epsilon^4 - 12\epsilon^2 \right) + t\epsilon - \sin(t\epsilon) \right]. \quad (\text{A1b})$$

For the $\sin(t/2)^2 \cos(t)$ in an time interval $t \in [0, 2\pi]$ they are

$$\alpha(t) = \frac{ig}{8} \left(\frac{e^{it(\epsilon-2)} - 1}{\epsilon - 2} - \frac{2(e^{it(\epsilon-1)} - 1)}{\epsilon - 1} + \frac{2(e^{it\epsilon} - 1)}{\epsilon} - \frac{2(e^{it(\epsilon+1)} - 1)}{\epsilon + 1} + \frac{e^{it(\epsilon+2)} - 1}{\epsilon + 2} \right), \quad (\text{A2a})$$

$$\theta(t) = \frac{g^2}{192\epsilon^2(\epsilon^4 - 5\epsilon^2 + 4)^2} \left\{ \epsilon(\epsilon^4 - 5\epsilon^2 + 4) \left[12t(7\epsilon^4 - 27\epsilon^2 + 8) + \epsilon^2 \left(8(5 - 2\epsilon^2) \sin(3t) + 3(\epsilon^2 - 1) \sin(4t) \right) \right. \right. \\ \left. \left. - 24(6\epsilon^4 - 23\epsilon^2 + 8) \sin(t) + 24(2\epsilon^4 - 7\epsilon^2 + 2) \sin(2t) \right] + 96\epsilon(\epsilon^2 + 2) \sin(t) (2(\epsilon^2 - 1) \cos(t) - \epsilon^2 + 4) \cos(t\epsilon) \right. \\ \left. - 48(\epsilon^2 + 2) \sin(t\epsilon) \left((\epsilon^2 - 1)(\epsilon^2 \cos(2t) + \epsilon^2 - 4) - 2\epsilon^2(\epsilon^2 - 4) \cos(t) \right) \right\}. \quad (\text{A2b})$$

Finally, for the $\sin(3t/2)^2$ modulation also for $t \in [0, 2\pi]$ they read,

$$\alpha(t) = \frac{g \left(-2(\epsilon^2 - 9) e^{it\epsilon} + (\epsilon - 3)\epsilon e^{it(\epsilon+3)} + (\epsilon + 3)\epsilon e^{it(\epsilon-3)} - 18 \right)}{4\epsilon(\epsilon^2 - 9)}, \quad (\text{A3a})$$

$$\theta(t) = \frac{g^2}{24\epsilon^2(\epsilon^2 - 9)^2} \left\{ (9 - \epsilon^2) \left[\epsilon^3 \sin(6t) + 4(9 - 2\epsilon^2)\epsilon \sin(3t) + 18 \left(t\epsilon(\epsilon^2 - 6) + 6 \sin(t\epsilon) \right) \right] \right. \\ \left. + 54(\epsilon - 3)\epsilon \sin(t(\epsilon + 3)) - 54\epsilon(\epsilon + 3) \sin(t(3 - \epsilon)) \right\}. \quad (\text{A3b})$$

In a similar fashion α and θ can be derived for the time

intervals of the sequences in Section IV.

[1] C. D. Bruzewicz, J. Chiaverini, R. McConnell, J. M. Sage, Trapped-ion quantum computing: Progress and

challenges, Appl. Phys. Rev. **6** (2): 021314 (2019).

- [2] I. Pogorelov et. al., Compact Ion-Trap Quantum Computing Demonstrator, *PRX Quantum* **2**, 020343 (2021).
- [3] C. Monroe et.al., Programmable quantum simulations of spin systems with trapped ions, *Rev. Mod. Phys.* **93**, 025001 (2021).
- [4] T. Manovitz, Y. Shapira, N. Akerman, A. Stern, and R. Ozeri, Quantum Simulations with Complex Geometries and Synthetic Gauge Fields in a Trapped Ion Chain *PRX Quantum* **1**, 020303 (2020).
- [5] T. Ilias, D. Yang, S. F. Huelga, and M. B. Plenio, Criticality-Enhanced Quantum Sensing via Continuous Measurement, *PRX Quantum* **3**, 010354 (2022).
- [6] Kevin A. Gilmore et al., Quantum-enhanced sensing of displacements and electric fields with two-dimensional trapped-ion crystals, *Science* **373**, 673-678 (2021).
- [7] A. D. Leu et.al., Fast, High-Fidelity Addressed Single-Qubit Gates Using Efficient Composite Pulse Sequences, *Phys. Rev. Lett.* **131**, 120601 (2023).
- [8] M. C. Smith, A. D. Leu, K. Miyaniishi, M. F. Gely, and D. M. Lucas, Single-qubit gates with errors at the 10^{-7} level, *arXiv:2412.04421 v1 [quant-ph]* (2024).
- [9] C. R. Clark et. al., High-Fidelity Bell-State Preparation with $^{40}\text{Ca}^+$ Optical Qubits, *Phys. Rev. Lett.* **127**, 130505 (2021).
- [10] J. P. Gaebler et.al., High-Fidelity Universal Gate Set for $^9\text{Be}^+$ Ion Qubits, *Phys. Rev. Lett.* **117**, 060505 (2016).
- [11] A. Sorensen and K. Molmer, Quantum Computation with Ions in Thermal Motion, *Phys. Rev. Lett.* **82**, 1971 (1999).
- [12] A. Sorensen and K. Molmer, Entanglement and quantum computation with ions in thermal motion, *Phys. Rev. A* **62**, 022311 (2000).
- [13] B. P. Ruzic et.al., Entangling-gate error from coherently displaced motional modes of trapped ions, *Phys. Rev. A* **105**, 052409 (2022).
- [14] D. Leibfried, B. DeMarco, V. Meyer, et al. Experimental demonstration of a robust, high-fidelity geometric two ion-qubit phase gate, *Nature* **422**, 412–415 (2003).
- [15] H. Hahn, G. Zarantonello, M. Schulte, et al. Integrated $^9\text{Be}^+$ multi-qubit gate device for the ion-trap quantum computer, *npj Quantum Inf* **5**, 70 (2019).
- [16] H. Takahashi et. al., Molmer-Sorensen entangling gate for cavity QED systems, *J. Phys. B: At. Mol. Opt. Phys.* **50** 195501 (2017).
- [17] A. Mitra, M. J. Martin, G. W. Biedermann, A. M. Marino, P. M. Poggi, and I. H. Deutsch, Robust Molmer-Sorensen gate for neutral atoms using rapid adiabatic Rydberg dressing, *Phys. Rev. A* **101**, 030301 (2020).
- [18] A.E. Webb, S.C. Webster, S. Collingbourne, D. Bretaud, A.M. Lawrence, S. Weidt, F. Mintert, and W.K. Hensinger, Resilient Entangling Gates for Trapped Ions, *Phys. Rev. Lett.* **121**, 180501 (2018).
- [19] Y. Shapira, R. Shani, T. Manovitz, N. Akerman, and R. Ozeri, Robust Entanglement Gates for Trapped-Ion Qubits, *Phys. Rev. Lett.* **121**, 180502 (2018).
- [20] M. Duwe, G. Zarantonello, N. Pulido-Mateo, H. Mendpara, L. Krinner, A. Bautista-Salvador, N. V. Vitanov, K. Hammerer, R.F. Werner and C. Ospelkaus, Numerical optimization of amplitude-modulated pulses in microwave-driven entanglement generation, *Quantum Sci. Technol.* **7** 045005 (2022).
- [21] G. Zarantonello, H. Hahn, J. Morgner, M. Schulte, A. Bautista-Salvador, R. F. Werner, K. Hammerer, and C. Ospelkaus, Robust and Resource-Efficient Microwave Near-Field Entangling $^9\text{Be}^+$ Gate, *Phys. Rev. Lett.* **123**, 260503 (2019).
- [22] M. Kang, Q. Liang, B. Zhang, S. Huang, Y. Wang, C. Fang, J. Kim, and K. R. Brown, Batch Optimization of Frequency-Modulated Pulses for Robust Two-Qubit Gates in Ion Chains, *Phys. Rev. Applied* **16**, 024039 (2021).
- [23] M. Kang, Y. Wang, C. Fang, B. Zhang, O. Khosravani, J. Kim, and K. R. Brown, Designing Filter Functions of Frequency-Modulated Pulses for High-Fidelity Two-Qubit Gates in Ion Chains, *Phys. Rev. Applied* **19**, 014014 (2023).
- [24] A. R. Milne, C. L. Edmunds, C. Hempel, F. Roy, S. Mavadia, and M. J. Biercuk, Phase-modulated entangling gates robust to static and time-varying errors, *Phys. Rev. Applied* **13**, 024022 (2020).
- [25] F. Haddadfarshi and F. Mintert, High fidelity quantum gates of trapped ions in the presence of motional heating, *New J. Phys.* **18** 123007 (2016).
- [26] Private communication with W.K. Hensinger.
- [27] Shi-Liang Zhu, C. Monroe and L.-M. Duan, Arbitrary-speed quantum gates within large ion crystals through minimum control of laser beams, *Europhys. Lett.* **73**, 485 (2006).
- [28] S. S. Ivanov and N. V. Vitanov, Composite two-qubit gates, *Phys. Rev. A* **92**, 022333 (2015).
- [29] R. T. Sutherland et. al., Versatile laser-free trapped-ion entangling gates, *New J. Phys.* **21** 033033 (2019).
- [30] C.J. Ballance, T.P. Harty, N.M. Linke, M.A. Sepiol, and D.M. Lucas, High-Fidelity Quantum Logic Gates Using Trapped-Ion Hyperfine Qubits, *Phys. Rev. Lett.* **117**, 060504 (2016).